Accessible solitons in complex Ginzburg-Landau media

Yingji He[1,2] and Boris A. Malomed[3]

[1]*School of Electronics and Information, Guangdong Polytechnic Normal University, 510665 Guangzhou, China*

[2]*Laboratory of Quantum Engineering and Quantum Materials, School of Physics and Telecommunication Engineering, South China Normal University, Guangzhou 510006, China*

[3]*Department of Physical Electronics, School of Electrical Engineering, Faculty of Engineering, Tel Aviv University, Tel Aviv 69978, Israel*

(Received 22 July 2013; published 18 October 2013)

We construct dissipative spatial solitons in one- and two-dimensional (1D and 2D) complex Ginzburg-Landau (CGL) equations with spatially uniform linear gain; fully nonlocal complex nonlinearity, which is proportional to the integral power of the field times the harmonic-oscillator (HO) potential, similar to the model of "accessible solitons;" and a diffusion term. This CGL equation is a truly nonlinear one, unlike its actually linear counterpart for the accessible solitons. It supports dissipative spatial solitons, which are found in a semiexplicit analytical form, and their stability is studied semianalytically, too, by means of the Routh-Hurwitz criterion. The stability requires the presence of both the nonlocal nonlinear loss and diffusion. The results are verified by direct simulations of the nonlocal CGL equation. Unstable solitons spontaneously spread out into fuzzy modes, which remain loosely localized in the effective complex HO potential. In a narrow zone close to the instability boundary, both 1D and 2D solitons may split into robust fragmented structures, which correspond to excited modes of the 1D and 2D HOs in the complex potentials. The 1D solitons, if shifted off the center or kicked, feature persistent swinging motion.

DOI: 10.1103/PhysRevE.88.042912 PACS number(s): 05.45.Yv, 42.65.Tg, 42.65.Sf

I. INTRODUCTION

Nonlocality naturally occurs in many settings in optics, plasmas, and Bose-Einstein condensates (BECs). Effects of nonlocal nonlinear dynamics with diverse correlation kernels have been studied in detail, both theoretically and experimentally, in optics [1] and in BECs, where the nonlocality is well known in the form of dipole-dipole interactions [2]. Nonlocal nonlinearities help to create various species of solitons [2,3], including fundamental ones [4,5], dipoles and vortices [5–7], multipeak states [8–10], and asymmetric solitons in couplers [11]. The nonlocality strongly affects interactions between solitons, too [12]. The nonlocal nonlinear response allows one to suppress the usual modulation instability of continuous waves. It also fosters the stabilization of diverse types of solitons in nonlocal media [13]. In addition to the use of self-focusing nonlocal nonlinearities, a possibility of supporting stable bright solitons by spatially inhomogeneous self-defocusing has been demonstrated recently, too [14].

Complex Ginzburg-Landau (CGL) equations represent a broad class of models which support spatial patterns due to the simultaneous balance of gain versus loss, and self-focusing nonlinearity versus diffraction or dispersion. CGL equations find numerous realizations in superconductivity and superfluidity, hydrodynamics and plasmas, reaction-diffusion systems, quantum field theory, and other physical contexts [15]. Well elaborated are applications of the CGL equations to nonlinear optics [16], where, in particular, they give rise to various species of dissipative solitons [17].

The above-mentioned ubiquity of nonlocal interactions makes it natural to consider CGL equations with nonlocal terms. Such equations were derived in diverse physical settings, including, in particular, combustion [18], the Faraday's parametric instability [19], electrochemistry [20], and waves of reaction-diffusion waves [21]. Various forms of nonlocal CGL equations were also proposed as mathematical models for the description of nonlinear-dissipative media with long-range interactions [22,23].

The ultimate form of the spatial nonlocal nonlinearity corresponds to the infinite correlation radius, i.e., the model with a constant kernel in the nonlocal term; see Eq. (1) below. The Schrödinger equation with such an ultranonlocal nonlinear term, multiplied by the harmonic-oscillator (HO) potential, was introduced by Snyder and Mitchell as a model of "accessible solitons" [24]. In terms of nonlocal CGL equations, the model with a flat kernel was proposed still earlier by Elmer [22]. A natural possibility is to study one- and two-dimensional (1D and 2D) dissipative solitons in the CGL equation with the same type of the ultimate nonlocality as in the Snyder-Mitchell model, but with a complex coefficient in front of this term, in which the imaginary part represents the nonlinear loss. This is the objective of the present paper. Our analytical considerations and numerical results reveal conditions for the existence of stable dissipative solitons in broad regions of the underlying parameter space. As concerns unstable solitons, they, generically, suffer spreading out into loosely bound fuzzy states. However, in narrow regions near instability boundaries, both 1D and 2D solitons split into robust fragmented clusters.

In addition, we study dynamical behavior of 1D solitons. It is demonstrated that a stable 1D soliton, initially shifted off the center, or suddenly kicked, performs a persistent swinging motion.

The rest of the paper is organized as follows. The ultranonlocal CGL equation is introduced in Sec. II, and the analytical framework for the study of dissipative solitons in this model is developed in Sec. III. Systematic results for the 1D and 2D solitons are reported in Sec. IV. The work is concluded by Sec. V.

II. MODEL

As said above, the model follows the general pattern of the extreme nonlocal nonlinearity which gives rise to the

accessible solitons in the 1D setting [24]:

$$iu_z = -\tfrac{1}{2}u_{xx} + gx^2u, \tag{1}$$

$$g = G\int_{-\infty}^{+\infty} |u(x)|^2 dx, \tag{2}$$

where, in terms of optical media, z and x are the propagation distance and transverse coordinate, and $G > 0$ is a constant. This type of the ultranonlocal nonlinearity can be naturally generalized for CGL equations in the following form, which is written here for the general 2D setting:

$$iu_z = \left(-\frac{1}{2} + i\beta\right)\nabla^2 u + [i\gamma_0 + (g - i\gamma_2)r^2]u, \tag{3}$$

$$\{g,\gamma_2\} = \{G,\Gamma\}\iint |u(x,y)|^2 dxdy \equiv \{G,\Gamma\}N, \tag{4}$$

where ∇^2 acts on transverse coordinates $\{x,y\}$, $r^2 \equiv x^2 + y^2$; $\beta \geqslant 0$ accounts for effective diffusion (viscosity); $\gamma_0 > 0$ is the linear-gain coefficient; and $\Gamma > 0$ represents nonlocal nonlinear dissipation.

The ultranonlocal nonlinearity assumed in Eqs. (1) and (2) can be realized in specially designed liquid-crystal optical waveguides [25]. The complex nonlinearity represented by Eq. (3) can be engineered similarly, if two-photon absorption, which is responsible for the imaginary part (γ_2), is taken into account (and enhanced by means of resonant dopants, if necessary). The diffusion term, which, as shown below, is necessary for the stability of dissipative solitons in the present model, appears if light creates free carriers in the medium, which undergo the diffusion (see, e.g., Ref. [26]).

Our intention is to construct stable localized solutions to the 1D and 2D versions of Eq. (3), which is possible despite the presence of the uniform linear gain, which usually makes all localized solutions unstable, as the respective zero background is obviously unstable. Recently, it was demonstrated that D-dimensional dissipative solitons can be made stable, in this case, if the coefficient in front of the local cubic loss term grows at $r \to \infty$ at any rate faster than r^D [27].

Because Eq. (3) looks like a linear Schrödinger equation with the complex HO potential, it is possible to construct 2D and 1D exact solutions in the form of isotropic chirped Gaussians (cf. Ref. [28], where such Gaussians were used as *Ansätze* for the variational approximation based on the corresponding complex Lagrangian):

$$u(r,z) = A(z)\exp\left\{-\frac{r^2}{2w^2(z)} + ic(z)r^2 + i\psi(z)\right\}, \tag{5}$$

(in the 1D case, radial coordinate r is replaced by the linear one, x), where variables $A(z)$, $w(z)$, c(z), and $\psi(z)$ represent the amplitude, width, wave-front curvature (chirp), and overall phase of the dissipative soliton, respectively. The integral power of *Ansatz* (5), defined according to Eq. (4), is

$$N = A^2(\sqrt{\pi}w)^D, \tag{6}$$

where $D = 1,2$ is the transverse dimension.

Note that Eq. (1) is only formally a nonlinear equation, being, in reality, fully tantamount to the linear Schrödinger equation, as it conserves the integral power. On the other hand, Eq. (3) gives rise to the following evolution equation for N:

$$\frac{dN}{dz} = 2\gamma_0 N - D\beta\left(\frac{1}{w^2} + 4c^2w^2\right)N - D\Gamma w^2 N^2, \tag{7}$$

whose feedback onto Eq. (3) makes it a truly nonlinear equation.

III. DISSIPATIVE SOLITONS

Inserting *Ansatz* (5) into Eq. (3), the following system of evolution equations for its parameters is derived in the exact form:

$$dA/dz = [\gamma_0 - D\beta w^{-2} - Dc]A, \tag{8a}$$

$$dw/dz = [\beta w^{-2} - 4\beta c^2 w^2 + 2c - \Gamma A^2(\sqrt{\pi}w)^D w^2]w, \tag{8b}$$

$$dc/dz = (2w^4)^{-1} - 2^{-(1+D/2)}A^2 w^{-2} - 4\beta c w^{-2} - 2c^2 - GA^2(\sqrt{\pi}w)^D. \tag{8c}$$

It is easy to check that the power-balance equation (7) is a corollary of Eq. (8).

Equations (8a)–(8c) give rise to a fixed-point (FP) solution, $A = A_0$, $w = w_0$ (i.e., $N = N_0$), and $c = c_0$, which can be found as a numerical solution of the respective algebraic system, obtained from Eq. (7) by setting the left-hand sides equal to zero. It is possible to derive an analytical approximation for the FP in the limit of weak gain, $\gamma_0 \to 0$. Even in this limit case, the general expressions are cumbersome; therefore we produce them for the situations when the loss is represented solely by the nonlinear term ($\beta = 0$, $\Gamma \neq 0$), or by the diffusion ($\Gamma = 0$, $\beta \neq 0$): At order γ_0 (next-order corrections are $\sim\gamma_0^2$),

$$\begin{aligned} w_0^{-2}(\beta = 0) &= \frac{2\gamma_0}{D\Gamma}(\sqrt{G^2+\Gamma^2} + G), \\ N_0(\beta = 0) &= \frac{4\gamma_0}{(D\Gamma)^2}(\sqrt{G^2+\Gamma^2} + G), \\ c_0(\beta = 0) &= \frac{\gamma_0}{D}, \end{aligned} \tag{9}$$

$$\begin{aligned} w_0^{-2}(\Gamma = 0) &= \frac{1}{D\beta}\left(1 + \frac{1}{\sqrt{1+4\beta^2}}\right), \\ N_0(\Gamma = 0) &= \frac{1+\sqrt{1+4\beta^2}}{(D\beta)^2 G}, \\ c_0(\Gamma = 0) &= -\frac{\gamma_0}{D\sqrt{1+4\beta^2}}. \end{aligned} \tag{10}$$

Note opposite signs of the chirp in FPs (9) and (10). Below, it is concluded that the FPs are unstable unless both the nonlinear loss and diffusion are present. Nevertheless, analytical results (9) and (10) are meaningful, as they demonstrate that the FPs exist at arbitrarily small values of the linear gain, rather than above any finite threshold.

Next, the stability of the FP can be investigated by introducing small perturbations about it, $A = A_0 + \Delta A(z)$, $w = w_0 + \Delta w(z)$, $c = c_0 + \Delta c(z)$, and deriving the respective

linearized equations:

$$d(\Delta a)/dz = b_1\Delta w + b_2\Delta c, \tag{11a}$$

$$d(\Delta w)/dz = b_3\Delta w + b_4\Delta c, \tag{11b}$$

$$d(\Delta c)/dz = b_5\Delta a + b_6\Delta w + b_7\Delta c, \tag{11c}$$

where we define $b_1 = 2A_0Dw_0^{-3}\beta$, $b_2 = -DA_0$, $b_3 = -(2\beta w_0^{-2} + 8\beta c_0^2 w_0^2 + 2\gamma_2 w_0^2)$, $b_4 = 2w_0 - 8c_0w_0^3\beta$, $b_5 = -A_0(2^{D/2}w_0^2)^{-1}$, $b_6 = -2w_0^{-1}[(2w_0^4)^{-1} + 2c_0^2 + GA^2(\sqrt{\pi}w)^D]$.

Solutions to Eq. (11) are looked for, as usual, with the z dependence in the form of $\exp(\lambda z)$, where the instability growth rate λ is determined by equating the determinant of the linearized system (11) to zero:

$$\begin{vmatrix} -\lambda & b_1 & b_2 \\ 0 & b_3-\lambda & b_4 \\ b_5 & b_6 & b_7-\lambda \end{vmatrix} = 0. \tag{12}$$

Thus, the FP solution to Eq. (8) is stable when roots of Eq. (12) have negative or zero real parts. Rewriting the equation in the form of $\lambda^3 + a_1\lambda^2 + a_2\lambda + a_3 = 0$, where $a_1 \equiv -(b_3 + b_7)$, $a_2 \equiv b_3b_7 - b_2b_5 - b_4b_6$, $a_3 \equiv b_5(b_2b_3 - b_1b_4)$, the stability condition amounts to the Routh-Hurwitz (RH) criterion, i.e., coefficients a_1, a_2, and a_3 must satisfy the system of three inequalities:

$$a_1 \geqslant 0, \quad \begin{vmatrix} a_1 & 1 \\ a_3 & a_2 \end{vmatrix} \geqslant 0, \quad \begin{vmatrix} a_1 & 1 & 0 \\ a_3 & a_2 & a_1 \\ 0 & 0 & a_3 \end{vmatrix} \geqslant 0.$$

These conditions actually reduce to a relatively simple system of inequalities:

$$a_1 \geqslant 0, \quad a_3 \geqslant 0, \quad a_1a_2 \geqslant a_3. \tag{13}$$

Similar stability criteria for stationary dissipative soliton solutions in CGL equations without an external potential [28], and with a linear potential [29], have been studied in detail before.

IV. RESULTS OF THE ANALYSIS

In addition to the numerical analysis of stability conditions (13) for the FP, the robustness of the soliton propagation was tested in direct simulations of the perturbed evolution of the respective dissipative solitons in the framework of Eq. (4). The direct simulations were initiated multiplying the wave form (5) by $1 + \rho(x,y)$, where $\rho(x,y)$ is a white-noise perturbation function, whose maximum was 10% of the soliton's amplitude.

A. The 1D case

Results produced by the FP-stability conditions (13) and direct simulations in the 1D setting are collected in Fig. 1. Quite naturally, the stability of dissipative solitons is most strongly affected by the linear-gain and diffusion coefficients, γ_0 and β. It is natural too that the solitons are stabilized by the increase of β and decrease of γ_0, and larger G, imposing a tighter nonlinearity-induced confinement, also helps to make the self-trapped modes more robust, extending their stability area in Fig. 1(a). Below the instability boundary, the soliton decays into a fuzzy but nevertheless loosely localized mode, as shown in Fig. 1(c). Some mismatch between the stability boundaries produced by the direct simulations and the RH

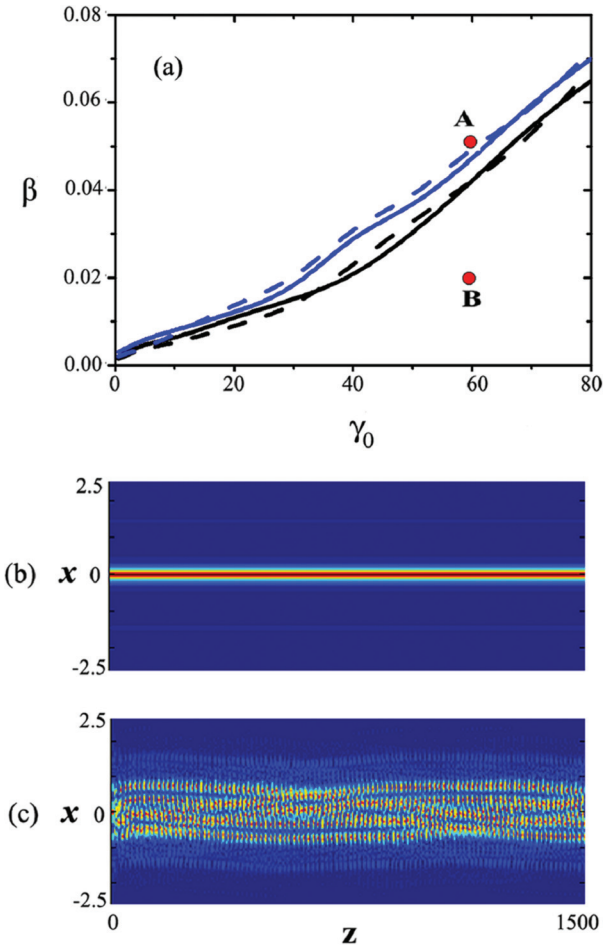

FIG. 1. (Color online) (a) The stability area for 1D dissipative solitons is located above the boundaries in the plane of the linear-gain and diffusion parameters (γ_0,β). The upper and lower curves correspond, respectively, to smaller and larger values of the nonlocality coefficient in Eq. (4), $G = 10$ and $G = 30$. The solid and dashed curves represent, severally, results collected from direct simulations of the perturbed evolution of the Gaussian dissipative soliton (5) within the framework of Eq. (3), and results produced by the FP-stability conditions (13). (b),(c) Examples of stable and unstable evolution of the solitons, respectively, for $\beta = 0.05$ [at point A in (a)] and $\beta = 0.02$ [at point B in (a)], while the other parameters are $G = 10$ and $\gamma_0 = 60$. In this figure, the nonlinear loss coefficient in Eq. (4) is fixed to be $\Gamma = 0.1$.

criterion is explained by the fact that the boundary revealed by the direct simulations corresponds to finite, rather than infinitesimal, perturbations.

Figure 1(a) shows that the stability of the solitons requires the presence of the diffusion term, $\beta > 0$, which is equally true at all values of other parameters. The analysis reveals that the stability is not possible either in the absence of the nonlinear loss (at $\Gamma = 0$) or confinement (at $G = 0$).

As shown in Fig. 2, in a narrow interval of values of the nonlocality coefficient G adjacent to the stability boundary, at $\beta < 0.04$, the instability can split the soliton into two symmetric fragments. This is an intermediate state between the stable solitons and fully unstable ones, which spread out into fuzzy modes. Plausibly, the stable split state may be realized as the first excited (odd) eigenmode in the effective

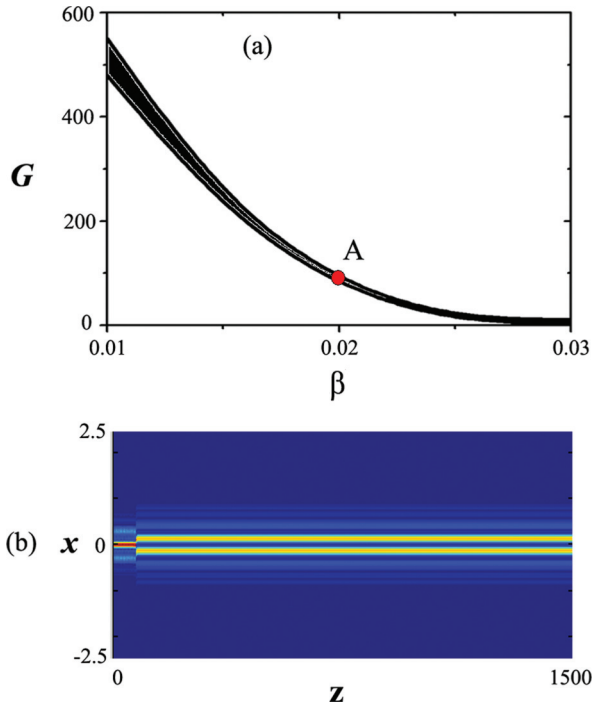

FIG. 2. (Color online) (a) The soliton splits into two fragments in the black strip in the plane of (β,G), while beneath the strip, the soliton decays into a fuzzy mode, similar to the one displayed in Fig. 1(c). (b) An example of the splitting for $G = 100$, $\gamma_0 = 60$, $\beta = 0.02$, and $\Gamma = 0.1$ [at point A in (a)].

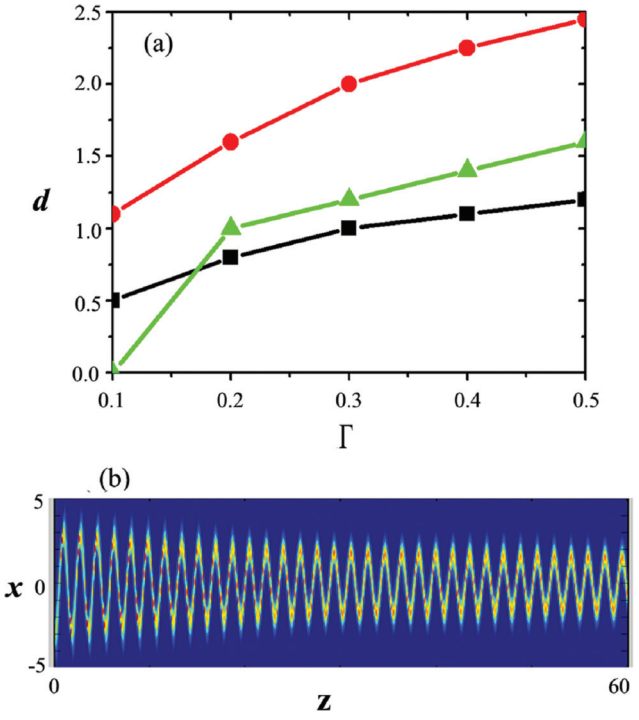

FIG. 3. (Color online) The swinging motion of the soliton. (a) The amplitude of the soliton's oscillations, d, versus the nonlocal nonlinear-dissipation coefficient, Γ, for three sets of parameters: circles ($G = 1$ and $\beta = 0.01$), triangles ($G = 1$ and $\beta = 0.02$), and squares ($G = 6$ and $\beta = 0.01$). (b) An example of the swinging motion with $\Gamma = 0.5$, $G = 6$, and $\beta = 0.01$, the input position of the soliton's center being $x_0 = 3$. In this figure, the linear-gain strength is $\gamma_0 = 13$.

1D complex HO potential, which can be identified in Eq. (3). In fact, the fuzzy mode displayed in Fig. 1(c) also features a nonvanishing intrinsic structure, which may be a consequence of the fact that the instability of the fundamental soliton is accounted for by a spontaneous transition into a higher excited state.

Simulations of the evolution of a soliton initially placed off the central point, $x = 0$, reveal its persistent swinging motion, in the effective HO potential, which sets in after a transient stage; see Fig. 3. The amplitude, d, of the established oscillations is chiefly determined by the nonlocal nonlinear-dissipation coefficient, Γ, as shown in Fig. 3(a). This phenomenon is similar to the soliton's swinging motion supported by spatially modulated losses, which was reported in Ref. [30]. Naturally, the amplitude of the oscillatory motion decreases with the increase of the diffusion coefficient, β, which induces effective viscosity (friction force) in the medium, as can be seen in Fig. 3(a), too—compare the circles for $\beta = 0.01$ and triangles for $\beta = 0.02$, both pertaining to $G = 1$. On the other hand, for fixed β, larger G implies the tighter confinement, also leading to a smaller amplitude of the oscillations—compare circles (for $G = 1$) and squares (for $G = 6$) in Fig. 3(a), both pertaining to $\beta = 0.01$.

Additional simulations (not shown here in detail) demonstrate that a similar dynamical regime can be initiated, instead of shifting the soliton off $x = 0$, by the application of a *kick* to it (i.e., by tilting the input beam, in terms of the optical waveguide).

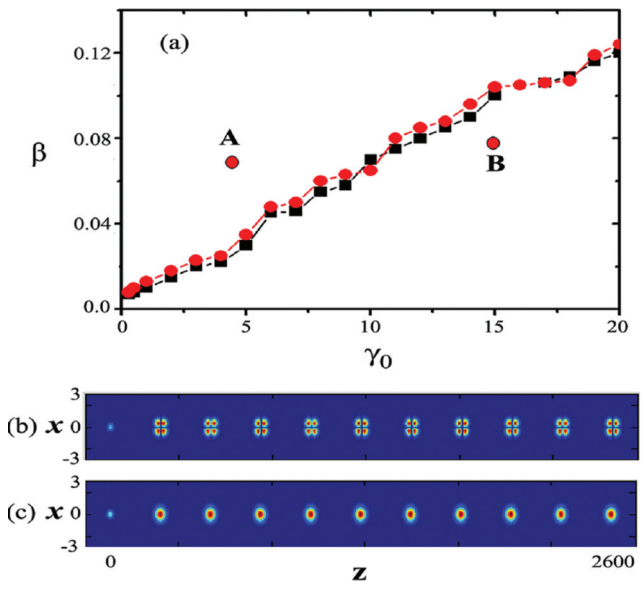

FIG. 4. (Color online) (a) The stability area for 2D dissipative solitons is located above the boundaries in the plane of the linear-gain and diffusion parameters (γ_0,β). The chains of circles and squares display, severally, results produced by the FP-stability conditions (13), and those collected from direct simulations of the perturbed evolution of the Gaussian dissipative soliton (5) within the framework of the 2D version of Eq. (3). Examples of unstable and stable perturbed evolution of the 2D solitons are displayed, respectively, in panel (b) for $\beta = 0.08$, $\gamma_0 = 16$ [point B in (a)] and in (c) for $\beta = 0.07$, $\gamma_0 = 8$ [point A in (a)]. In this figure, $G = 4$ and $\Gamma = 0.1$.

B. The 2D case

The stability chart for the 2D solitons, displayed in Fig. 4(a), is qualitatively similar to its 1D counterpart; cf. Fig. 1(a). In particular, the increase of the diffusion coefficient, β, and decrease of the linear gain, γ_0, lead to the expansion of the stability area. Also similar to the 1D situation is the conclusion that 2D solitons cannot be stable when any of the coefficients β, Γ, G vanishes [in particular, Fig. 4(a) clearly demonstrates that the presence of the diffusion term with $\beta > 0$ is necessary for the stability].

An example of the unstable evolution in Fig. 4(b) demonstrates that the instability can split the 2D soliton into multiple fragments, similar to the splitting of the 1D soliton in Fig. 2. In an appropriate parameter region, the fragmented cluster may feature robust propagation, as observed in Fig. 4(b). It is plausible that the cluster corresponds to an excited state of the 2D HO in the isotropic complex potential.

Another feature of the 2D setting, which is qualitatively similar to what was reported above for the 1D solitons, is the fact that the stable fragmented clusters exist in a relatively narrow intermediate zone, at $\beta < 0.04$, between stable solitons and unstable ones decaying into a loosely bound fuzzy mode, as shown in Fig. 5 in the plane of (β, G). The tapering and eventual vanishing of the splitting zone in Fig. 5(a), following the growth of G and decrease of β, which makes it different from the shape of the splitting zone in the 1D setting [cf. Fig. 2(a)], is explained by suppression of the splitting in the limit of large G and small β, i.e., in the nearly conservative model, under the action of the surface tension. Naturally, the solitons tend to become more stable for the stronger confinement and viscosity; therefore the stability region, III in Fig. 5(a), expands with the increase of G and β, similar to what is observed in Fig. 2(a) in the 1D setting.

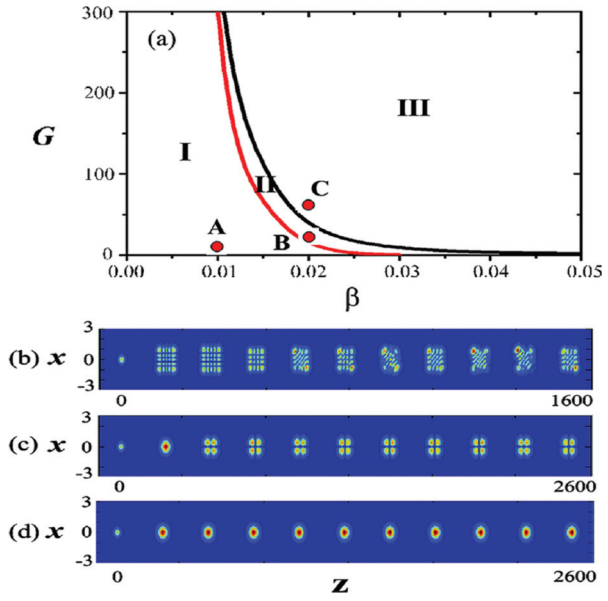

FIG. 5. (Color online) (a) The stability chart for 2D solitons in the plane of the diffusion coefficient, β, and nonlocal-nonlinearity strength, G. In region I the 2D solitons decay into fuzzy modes [an example is displayed in (b) for $G = 5$ and $\beta = 0.01$, which corresponds to point A in (a)]. In narrow zone II, the soliton splits into a robust fragmented cluster; see an example in (c) for $G = 20$ and $\beta = 0.02$, which corresponds to point B in (a). It is similar to the stable cluster which is displayed, for other values of the parameters, in Fig. 4(b). The 2D solitons are stable in region III; see an example in (d) for $G = 55$ and $\beta = 0.02$, which corresponds to point C in (a) [cf. another example of the stable 2D soliton displayed in Fig. 4(c)]. In this figure, $\Gamma = 0.1$ and $\gamma_0 = 4$.

Completely unstable 2D solitons spread out into a loosely confined fuzzy state, as shown in Fig. 5(b), which is also similar to the instability of 1D solitons; cf. Fig. 1(c). It is worthy to note that the 2D fuzzy mode keeps the overall rectangular shape, and simulations on a much longer scale of z (not shown here in detail) do not demonstrate a transformation of the fuzzy mode into a more circular form, which might be expected due to the axial symmetry of Eq. (3). The persistence of the internal structure of the 2D fuzzy mode may be a consequence of the fact that the instability is accounted for by a spontaneous transition of the fundamental soliton into a higher-order excited mode; cf. the similar situation in the 1D setting [Fig. 1(c)].

On the other hand, in contrast to the 1D setting, which admits the swinging motion of the solitons (Fig. 3), in the 2D model the soliton initially placed off the center, or suddenly kicked, does not feature persistent oscillations, but is quickly pulled back to the central position (not shown here in detail); i.e., the effective viscous friction acting on the 2D soliton is much stronger than in 1D.

V. CONCLUSIONS

We have introduced the CGL extension of the ultranonlocal Snyder-Mitchell model for the accessible solitons, in both the 1D and 2D forms. Unlike the actually linear Schrödinger equation in the original model, the present nonlocal CGL equation is a truly nonlinear one, due to the feedback of the evolution of the total norm, according to Eq. (7). Stationary solutions for the 1D and 2D dissipative solitons were found in the semiexplicit form, and their stability was analyzed semiexplicitly, too, by means of the RH criterion. The stability was also verified via direct simulations. Unstable solitons decay into fuzzy modes, which remain loosely bound, under the action of the complex HO potential. In narrow zones adjacent to the stability boundary, the solitons split into robust fragmented clusters, which may be realized as excited states of the 1D or 2D harmonic oscillator. The stability of the dissipative solitons demands the simultaneous presence of the nonlocal nonlinear confinement and loss, and of the diffusion term.

The model can be implemented in optics—in particular, using nonlocal liquid-crystal media. It may be interesting to extend the analysis of the 2D setting, with the aim to construct vortex modes and test their stability (similarly, it may be possible to construct antisymmetric twisted modes in 1D). In terms of the 2D model, it may also be interesting to generalize the analysis for anisotropic CGL equations; cf. Ref. [31].

ACKNOWLEDGMENTS

This work was supported by the National Natural Science Foundation of China (Grant No. 11174061) and the Guangdong Province Natural Science Foundation (Grants No. S2011010005471 and No. S2013010015795).

[1] W. Królikowski, O. Bang, N. I. Nikolov, D. Neshev, J. Wyller, J. J. Rasmussen, and D. Edmundson, J. Opt. B: Quantum Semiclassical Opt. **6**, S288 (2004); Z. Chen, M. Segev, and D. N. Christodoulides, Rep. Prog. Phys. **75**, 086401 (2012); M. Peccianti and G. Assanto, Phys. Rep. **516**, 147 (2012).

[2] T. Lahaye, C. Menotti, L. Santos, M. Lewenstein, and T. Pfau, Rep. Prog. Phys. **72**, 126401 (2009).

[3] C. Conti, M. Peccianti, and G. Assanto, Phys. Rev. Lett. **91**, 073901 (2003).

[4] Q. Guo, B. Luo, F. Yi, S. Chi, and Y. Xie, Phys. Rev. E **69**, 016602 (2004).

[5] C. Rotschild, O. Cohen, O. Manela, M. Segev, and T. Carmon, Phys. Rev. Lett. **95**, 213904 (2005).

[6] A. I. Yakimenko, Y. A. Zaliznyak, and Y. Kivshar, Phys. Rev. E **71**, 065603(R) (2005).

[7] Y. J. He, B. A. Malomed, D. Mihalache, and H. Z. Wang, Phys. Rev. A **78**, 023824 (2008); **77**, 043826 (2008); F. Ye, B. A. Malomed, Y. He, and B. Hu, *ibid.* **81**, 043816 (2010).

[8] A. V. Mamaev, A. A. Zozulya, V. K. Mezentsev, D. Z. Anderson, and M. Saffman, Phys. Rev. A **56**, R1110 (1997).

[9] S. Lopez-Aguayo, A. S. Desyatnikov, Y. S. Kivshar, S. Skupin, and W. Królikowski, Opt. Lett. **31**, 1100 (2006); Y. V. Kartashov, L. Torner, V. A. Vysloukh, and D. Mihalache, *ibid.* **31**, 1483 (2006).

[10] I. Kaminer, C. Rotschild, O. Manela, and M. Segev, Opt. Lett. **32**, 3209 (2007).

[11] X. Shi, B. A. Malomed, F. Ye, and X. Chen, Phys. Rev. A **85**, 053839 (2012).

[12] M. Peccianti, K. A. Brzdakiewicz, and G. Assanto, Opt. Lett. **27**, 1460 (2002).

[13] O. Bang, W. Królikowski, J. Wyller, and J. J. Rasmussen, Phys. Rev. E **66**, 046619 (2002).

[14] Y.-J. He and B. A. Malomed, Phys. Rev. A **87**, 053812 (2013).

[15] M. Ipsen, L. Kramer, and P. G. Sorensen, Phys. Rep. **337**, 193 (2000); I. S. Aranson and L. Kramer, Rev. Mod. Phys. **74**, 99 (2002); M. van Hecke, Physica D **174**, 134 (2003); B. A. Malomed, in *Encyclopedia of Nonlinear Science*, edited by A. Scott (Routledge, New York, 2005), p. 157.

[16] M. E. Fermann, A. Galvanauskas, G. Sucha, and D. Harter, Appl. Phys. B **65**, 259 (1997); F. T. Arecchi, S. Boccaletti, and P. Ramazza, Phys. Rep. **318**, 1 (1999); F. S. Ferreira, M. M. V. Facao, and S. C. V. Latas, Fiber Integr. Opt. **19**, 31 (2000); P. Mandel and M. Tlidi, J. Opt. B: Quantum Semiclassical Opt. **6**, R60 (2004); N. N. Rosanov, S. V. Fedorov, and A. N. Shatsev, Appl. Phys. B **81**, 937 (2005); C. O. Weiss and Ye. Larionova, Rep. Prog. Phys. **70**, 255 (2007); N. Akhmediev, J. M. Soto-Crespo, and P. Grelu, Chaos **17**, 037112 (2007); B. A. Malomed, *ibid.* **17**, 037117 (2007).

[17] *Dissipative Solitons*, edited by N. Akhmediev and A. Ankiewicz (Springer, Berlin, 2005).

[18] B. J. Matkowsky and V. Volpert, Physica D **54**, 203 (1992).

[19] M. Higuera, J. Porter, and E. Knobloch, Physica D **162**, 155 (2002).

[20] V. Garcia-Morales and K. Krischer, Phys. Rev. Lett. **100**, 054101 (2008).

[21] D. Lima, D. Battogtokh, A. Mikhailov, P. Borckmans, and G. Dewel, Europhys. Lett. **42**, 631 (1998); D. Tanaka and Y. Kuramoto, Phys. Rev. E **68**, 026219 (2003); A. S. Mikhailov and K. Showalter, Phys. Rep. **425**, 79 (2006).

[22] F. J. Elmer, Physica D **30**, 321 (1988); Phys. Rev. A **41**, 4174 (1990).

[23] A. Doelman and V. Rottschafer, J. Nonlinear Sci. **7**, 371 (1997); J. Norbury, J. C. Wei, and M. Winter, Nonlinearity **15**, 2077 (2002); V. A. Volpert, A. A. Nepomnyashchy, L. G. Stanton, and A. A. Golovin, SIAM J. Appl. Dyn. Sys. **7**, 265 (2008).

[24] A. W. Snyder and D. J. Mitchell, Science **276**, 1538 (1997).

[25] I. B. Burgess, M. Peccianti, G. Assanto, and R. Morandotti, Phys. Rev. Lett. **102**, 203903 (2009).

[26] O. Hess and T. Kuhn, Phys. Rev. A **54**, 3360 (1996).

[27] O. V. Borovkova, Y. V. Kartashov, V. A. Vysloukh, V. E. Lobanov, B. A. Malomed, and L. Torner, Opt. Express **20**, 2657 (2012).

[28] V. Skarka and N. B. Aleksić, Phys. Rev. Lett. **96**, 013903 (2006); N. B. Aleksić, V. Skarka, D. V. Timotijevic, and D. Gauthier, Phys. Rev. A **75**, 061802(R) (2007); V. Skarka, N. B. Aleksić, H. Leblond, B. A. Malomed, and D. Mihalache, Phys. Rev. Lett. **105**, 213901 (2010); B. Aleksić, B. Zarkov, V. Skarka, and N. Aleksić, Phys. Scr. **T149**, 014037 (2012).

[29] W.-L. Zhu and Y.-J. He, Opt. Express **18**, 17053 (2010).

[30] Y. He and D. Mihalache, J. Opt. Soc. Am. B **29**, 2554 (2012); Phys. Rev. A **87**, 013812 (2013).

[31] M. Falcke, H. Engel, and M. Neufeld, Phys. Rev. E **52**, 763 (1995).